

Sea Level Change, Anaerobic Methane Oxidation, and the Glacial-Interglacial Phosphorus Cycle

Bjorn Sundby¹, Alfonso Mucci¹, Pascal Lecroart², and Pierre Anschutz²

¹McGill University

²Université de Bordeaux

November 22, 2022

Abstract

The oceanic phosphorus cycle describes how phosphorus moves through the ocean, accumulates with the sediments on the sea floor, and participates in biogeochemical reactions. We propose a new two-reservoir scenario of the glacial-interglacial phosphorus cycle. It relies on diagenesis in methane hydrate-bearing sediments to mobilize sedimentary phosphorus and transfer it to the ocean during times when falling sea level lowers the hydrostatic pressure on the sea floor and destabilizes methane hydrate. Throughout the cycle, primary production assimilates phosphorus and inorganic carbon into biomass which, upon settling and burial, returns phosphorus to the sedimentary reservoir. The impact of the two processes is not balanced: the former increases the oceanic phosphorus inventory whereas the latter decreases it. Primary production also lowers the partial pressure of CO₂ in the surface ocean, potentially drawing down CO₂ from the atmosphere. Concurrent with this slow ‘biological pump’, but operating in the opposite direction, a ‘physical pump’ brings metabolic CO₂-enriched waters from deep-ocean basins to the upper ocean. The two pumps compete, but the direction of the CO₂ flux at the air-sea interface depends on the nutrient content of the deep waters. Because of the transfer of reactive phosphorus to the sediment throughout a glaciation cycle, low phosphorus/high CO₂ deep waters reign in the beginning of the deglaciation, resulting in rapid transfer of CO₂ to the atmosphere. The new scenario provides another element to the suite of processes that may have contributed to the rapid glacial-interglacial climate transitions documented in paleo records.

Hosted file

06 table 1. chronology of events .docx available at <https://authorea.com/users/533357/articles/598172-sea-level-change-anaerobic-methane-oxidation-and-the-glacial-interglacial-phosphorus-cycle>

1 Sea Level Change, Anaerobic Methane Oxidation, and the Glacial- 2 Interglacial Phosphorus Cycle

3
4 Bjorn Sundby^{1,2}, Pierre Anschutz³, Pascal Lecroart³, and Alfonso Mucci²

5
6 ¹ISMER, Université du Québec à Rimouski, Rimouski, QC, Canada H4C 3J9; ²GEOTOP and Earth&
7 Planetary Sciences, McGill University, Montreal, QC, Canada H3A 0E8; ³EPOC, Université de Bordeaux,
8 33615 Pessac, France.

9
10 Correspondance to: Bjorn Sundby (bjorn.sundby@mcgill.ca)

11
12
13 **ABSTRACT** The oceanic phosphorus cycle describes how phosphorus moves through the ocean,
14 accumulates with the sediments on the sea floor, and participates in biogeochemical reactions. We
15 propose a new two-reservoir scenario of the glacial-interglacial phosphorus cycle. It relies on
16 diagenesis in methane hydrate-bearing sediments to mobilize sedimentary phosphorus and
17 transfer it to the ocean during times when falling sea level lowers the hydrostatic pressure on the
18 sea floor and destabilizes methane hydrate. Throughout the cycle, primary production assimilates
19 phosphorus and inorganic carbon into biomass which, upon settling and burial, returns
20 phosphorus to the sedimentary reservoir. The impact of the two processes is not balanced: the
21 former increases the oceanic phosphorus inventory whereas the latter decreases it. Primary
22 production also lowers the partial pressure of CO₂ in the surface ocean, potentially drawing down
23 CO₂ from the atmosphere. Concurrent with this slow 'biological pump', but operating in the
24 opposite direction, a 'physical pump' brings metabolic CO₂ enriched waters from deep-ocean
25 basins to the upper ocean. The two pumps compete, but the direction of the CO₂ flux at the air-sea
26 interface depends on the nutrient content of the deep waters. Because of the transfer of reactive
27 phosphorus to the sediment throughout a glaciation cycle, low phosphorus/ high CO₂ deep waters
28 reign in the beginning of the deglaciation, resulting in rapid transfer of CO₂ to the atmosphere. The
29 new scenario provides another element to the suite of processes that may have contributed to the
30 rapid glacial-interglacial climate transitions documented in paleo records.

31 32 33 **Key Points**

34 *A 2-reservoir scenario of the oceanic P-cycle predicts that the oceanic P- inventory expands during the
35 onset of a glaciation but contracts and reaches its lower limit during the deglaciation.

36 *The scenario predicts that transfer of phosphorus from the oceanic to the sedimentary P-reservoir
37 weakens the power of the biological nutrient pump to draw down atmospheric CO₂.

38 *Upwelling of nutrient poor water near the end of a glaciation takes control of outgassing and produces
39 a spike in the atmospheric CO₂.

40 **Keywords:** diagenesis; methane; gas hydrate; carbon dioxide; SMT-sulfate methane transition zone;
41 atmosphere

42 1. INTRODUCTION

43 Each of the glacial cycles that characterize the Pleistocene lasted roughly 100 Kyr. During each
44 cycle, about 90 Kyr were glacial (cold), allowing continental ice sheets to build up, and 10 Kyr were
45 interglacial (warm), allowing the ice to melt. The large volumes of water transferred from the ocean to
46 the continents during the glacial part of the cycle and the return flow of water to the ocean during the
47 interglacial caused the globally-averaged sea level to fall by more than 100 meters and then rise again
48 (e.g. Siddal et al., 2003; Lambeck et al., 2014). Seasonality changes, caused by cyclic variations in
49 Earth's orbit around the Sun (Milankovitch cycles), are the fundamental drivers of the glacial cycles, but
50 orbital variations by themselves cannot account for the rapid climate transitions documented in paleo-
51 records. This implies that positive feedbacks within Earth's climate system must amplify the orbital
52 driver (Sigman & Boyle, 2000). Much research has focused on processes that might provide such
53 feedbacks. Since carbon dioxide (CO₂) is a greenhouse gas and since the ocean is the largest CO₂
54 reservoir on Earth (fifty times larger than the atmospheric reservoir), processes that influence the
55 exchange of CO₂ between the ocean and the atmosphere top the list of candidates.

56 Measurements on air samples trapped in ice cores have shown that the partial pressure of CO₂
57 (pCO₂) in the atmosphere during the glacial period of a cycle was substantially lower than during the
58 intervening interglacial (Barnola et al., 1987; Petit et al., 1999). The atmospheric pCO₂ decreased slowly
59 throughout the glacial part of the cycle, as did sea-level. By comparison, both the rise of atmospheric
60 pCO₂ and the rise of the sea level at the end of the glaciation (termination) were remarkably rapid,
61 lasting 10 Kyr or less. The similarity between the sea-level change and the change in atmospheric pCO₂
62 through time suggests that the two phenomena are linked, but the nature of the link has remained elusive
63 (e.g. Sigman & Boyle, 2000; Kohfeld et al., 2005; Peacock et al., 2006; Sigman et al., 2010).

64 Another greenhouse gas, methane, is abundant in continental margin sediments where it occurs
65 as a solid in the form of methane hydrate (clathrate) (Kvenvolden, 1993; Bohrmann & Torres, 2006;
66 Ruppel & Kessler, 2017). Paull et al. (1991) proposed a direct link between sea level fall and global
67 warming as follows: As the sea level falls, the pressure on the sediment column decreases, methane
68 hydrate become destabilized, and methane gas is released into the pore water. They further proposed that
69 methane released in this way could reach the atmosphere and initiate a warming event, but it is doubtful
70 that the vast quantities of methane that would be required to trigger substantial warming could reach the
71 atmosphere before being oxidized in the sediments and the overlying water (Archer et al., 2000; Archer,

72 2007). The search for mechanisms that may explain the glacial-interglacial variation in atmospheric
73 pCO₂ has therefore focused on other scenarios.

74 Common to many scenarios is the idea that the whole ocean inventory of major nutrients may
75 have varied on glacial-interglacial time scales: If the nutrient inventory in the global ocean were to
76 increase, mixing and upwelling could increase the flux of nutrients to the surface ocean. This would
77 stimulate primary productivity, increase the flux of organic matter to the seafloor, and lower the pCO₂ in
78 the surface ocean. If the pCO₂ in the surface ocean were to fall below the atmospheric pCO₂, CO₂ would
79 be drawn down from the atmosphere. A temporally variable nutrient inventory could thus explain the
80 glacial-interglacial pCO₂ difference. The combination of processes involved in this scenario has become
81 known as the biological pump (e.g. Falkowski, 1997; Hain et al., 2014).

82 Searching for a temporary sink for phosphorus, the nutrient often considered to be limiting on
83 geological time scales, Broecker (1982a, 1982b) developed a scenario whereby phosphorus is removed
84 from the global ocean by deposition of P-containing sediment on continental shelves during sea-level
85 high stands and returned to the ocean by erosion of shelf sediments during sea-level low stands. This
86 scenario, which is known as the “shelf nutrient hypothesis” suffers a major weakness: The amount of
87 sediment that has to be deposited and eroded on the relevant time scale appears to be far greater than can
88 be supported by observations (Peacock et al., 2006). Another weakness of the hypothesis is the absence
89 of an explicit mechanism that would release phosphate into the aqueous phase once the sediments are
90 eroded. Indeed, as Archer et al. (2000) stated, it seems that all of the simple mechanisms for lowering
91 pCO₂ in the surface ocean have been eliminated. Broecker (2018) made the point that although alternate
92 scenarios may exist to explain glacial cycles, one must take into account that the situation is complex,
93 and that no single scenario may be the ‘best’.

94

95 **2. OBJECTIVES AND APPROACH**

96 In a recent modeling study, we drew attention to the fact that methane is a fuel that can drive
97 diagenesis in sediments. Using manganese as an example, we showed that methane-fuelled diagenesis
98 can reduce and redistribute solid-phase oxidized manganese throughout the sediment column (Sundby et
99 al., 2015). Building on that study, we now focus on methane-fuelled reduction of oxidized sedimentary
100 iron-phases and the consequent release of iron oxide-bound phosphorus into the pore water. The
101 objective is to develop a chronological scenario of phosphorus cycling in the global ocean over a full
102 glacial cycle. In this scenario, which capitalizes on the two-reservoir model of Broecker (1982a, 1982b),

103 phosphorus cycles between two principal reservoirs: the ocean and the sediments that accumulate on
104 continental margins.

105 We focus on the mechanisms that promote the release of sedimentary phosphorus into the pore
106 waters and the transfer of phosphorus to the oceanic reservoir. We then explore the mechanisms that
107 return phosphorus to the sedimentary reservoir throughout a glacial cycle. Finally, we examine the
108 interaction of the glacial-interglacial phosphorus cycle with the carbon system to discover how this
109 interaction might affect variations in atmospheric pCO₂. The approach focuses on large scale temporal
110 and spatial processes, but it does not preclude eventual incorporation of shorter timescale and broader
111 spatial-scale processes in a more detailed scenario. By including diagenesis, we can revive elements of
112 Broecker's original hypothesis by providing a set of mechanisms that do not rely on large scale erosion
113 to release phosphate from sediments. We will also re-examine the idea proposed by Paull et al. (1991,
114 2002) that sedimentary methane may be directly involved in the atmospheric carbon cycle by escaping
115 to the atmosphere during periods of sea-level fall. By invoking diagenesis (anaerobic methane oxidation
116 produces sulfide that reduces iron oxides and releases soluble phosphate into pore waters) we can show
117 that methane plays an indirect but essential role in the redistribution of phosphate between the oceanic
118 and the sedimentary reservoirs.

119

120 **3. DIAGENESIS AND FLUXES OF PHOSPHORUS IN CONTINENTAL MARGIN** 121 **SEDIMENTS**

122

123 *3.1 Sources and sinks of phosphorus.* The inventory of the oceanic phosphorus reservoir
124 depends on the supply of phosphorus from the continents, remineralization of organic phosphorus in the
125 water column and the upper sediment column, burial of solid phases with which phosphorus is
126 associated, release of soluble phosphorus from the sediments, and removal by hydrothermal activity (e.g.
127 Wallmann, 2010). Burial on the abyssal seafloor is the ultimate sink for phosphorus, but an amount
128 equivalent to about half of the total phosphorus flux from the continents to the modern ocean does not
129 reach the abyssal seafloor but settles out and is buried on continental margins (Colman & Holland, 2000;
130 Ruttenger, 2003). The particulate phosphorus that is delivered to the seafloor contains, on average, one
131 third each of organic phosphorus, iron oxide-bound phosphorus, and poorly - reactive apatite minerals
132 (Delaney, 1998; Fillipelli, 1997; Ruttenger, 2003). Organic phosphorus exists in a variety of forms
133 (primarily phosphate esters) that originate from excretion, decomposition, death, and autolysis of
134 organisms. Microbial degradation of organic matter during the earliest stages of diagenesis converts

135 organic phosphorus to dissolved inorganic phosphate. Part of the remineralized phosphorus escapes into
136 the water column and is added to the oceanic phosphorus reservoir; part of it is co-precipitated with or
137 adsorbed onto iron (hydr)oxide minerals or may be converted to poorly reactive phases such as calcium
138 fluoroapatite (Delaney, 1998).

139 In its simplest expression, the marine phosphorus cycle consists of a source and a sink of P-
140 bearing material and a set of processes that act upon this material (figure 1). Erosion and weathering of
141 continental rocks supply phosphorus to the ocean, and burial on the sea floor removes it. Until recently,
142 the phosphorus sink was thought to be represented by poorly reactive (stable) apatite minerals. This
143 view had presumably its origin in the analytical procedures that were used to quantify individual P-
144 containing components in marine sediments. This view is now changing, and other phosphorus minerals
145 are thought to be involved. This is exemplified by autogenesis of vivianite, a hydrous ferrous phosphate
146 that can form in sulfate poor sediments such as those in brackish estuaries. Egger et al. (2015) suggested
147 that vivianite may act as an important burial sink for phosphorus in brackish environments worldwide.
148 Vivianite authigenesis requires porewater with elevated ferrous iron (Fe^{2+}) and phosphate
149 concentrations (e.g. Liu et al., 2018). Low-sulfate lacustrine settings typically satisfy these criteria, and
150 vivianite is commonly reported from freshwater sediments (e.g., Rothe et al., 2014).

151 In more sulfate-rich settings, the presence of a sulfate–methane transition zone (SMT) has been
152 shown to provide favourable conditions for vivianite authigenesis (Egger et al., 2015a, 2016; Hsu et al.,
153 2014; März et al., 2008a, 2018; Slomp et al., 2013). The production of dissolved sulfide by anaerobic
154 oxidation of methane (and the associated conversion of Fe-oxides to Fe-sulfides, result in elevated
155 porewater PO_4 concentrations around the SMT (März et al., 2008a). The subsequent downward
156 diffusion of PO_4 into sulfide-depleted porewater below the SMTZ may lead to precipitation of vivianite
157 if sufficient reduced Fe is available (e.g., Egger et al., 2015a; März et al., 2018).

158 Porewater profiles of phosphate in marine sediments tend to display a concentration maximum
159 within or near the sulfate methane transition zone (SMT) (e.g. März et al., 2008a). The associated
160 concentration gradients imply vertical transport of soluble phosphate both in the downward and the
161 upward direction. To sustain these fluxes requires the presence of phosphate sinks both below as well as
162 above the SMT zone. This conclusion is in agreement with the postulated presence of a phosphate sink
163 and its strength, but it does not provide information about the nature of the sink.

164 A large body of research shows that phosphate is in fact released from continental margin
165 sediments into the overlying oceanic water. Perhaps the most prominent result of this research is the
166 paper by Colman and Holland (2000). They analyzed nearly 200 published porewater profiles of
167 dissolved phosphate in sediment cores from a variety of marine environments and calculated phosphate
168 fluxes into the overlying water. They concluded that the return flux of phosphate from margin sediment
169 was more than one order of magnitude larger than the riverine flux of total dissolved phosphorus
170 towards the ocean. Wallmann (2010) used a mass balance approach to estimate phosphate fluxes in the
171 ocean and came up with the remarkable conclusion that the pre-human modern ocean is losing dissolved
172 phosphate (to the sedimentary reservoir) at a rate of about 5% Kyr⁻¹. Studies of phosphorus diagenesis
173 in continental margin sediments have also shown that phosphate is released to the overlying waters
174 (Sundby et al., 1992). These observations point to the important role that diagenesis (oxidation of
175 reduced carbon) plays in the marine phosphorus cycle. Methane being prominently present in
176 continental margin sediments suggests that our scenario, whereby sea level variations have important
177 consequences for methane oxidation, has merit. Beyond the data, the next step could well be a better
178 quantification of methane-fuelled diagenesis, but we are not convinced that the understanding of
179 phosphorus and iron reservoirs, processes, and boundary conditions have progressed to the point where
180 we are ready to attempt meaningful modelling of the oceanic phosphorus cycle.

181

182 **3.2 Phosphorus diagenesis.** The term *phosphorus* usually stands for the sum total of all
183 phosphorus species, organic as well as inorganic, particulate as well as dissolved. It is typically defined
184 operationally according the analytical methods by which it is determined (e.g., Poulton and Canfield,
185 2006; Ruttenberg, 2003). Phosphorus bound to iron oxides is defined operationally as “reactive
186 particulate phosphorus” but the latter definition typically includes particulate organic phosphorus,
187 phosphate reversibly adsorbed to other mineral surfaces, as well as phosphate in carbonate fluorapatite
188 minerals and fish bones. In sediment pore waters, soluble reactive phosphorus (also referred to as
189 orthophosphate or dissolved inorganic phosphorus) is a minor component of the reactive phosphorus
190 pool and occurs chiefly as the hydrogen phosphate species (HPO_4^{2-}). Particulate and soluble forms of
191 phosphorus are subjected to different modes of transport. Particulate phosphorus is transported to the
192 sea floor by settling through the oceanic water column and is buried in the sediment. Soluble forms of
193 phosphorus are transported by diffusion along concentration gradients that often develop in sediment
194 pore waters. Transport via bioirrigation can be important in the upper sediment column.

195 In this study we refer to soluble inorganic phosphorus as “*phosphate*” and to insoluble forms as
196 “*particulate phosphorus*” or “*total phosphorus*”. The term *reactive iron* has been applied to the fraction
197 of iron in marine sediments that reacts readily with sulfide (Canfield, 1989). By analogy, we define
198 *reactive particulate phosphorus* as the fraction of total P that is adsorbed on or is co-precipitated with
199 iron oxides and can therefore be released to pore waters when iron oxides are reductively dissolved.
200 The challenge presented by the original shelf nutrient scenario is to find mechanisms that can trigger
201 reciprocal changes in the sedimentary and oceanic phosphorus inventories over a glacial cycle.
202 Diagenesis is a strong candidate for such a mechanism. Diagenesis is defined as the sum of the physical,
203 chemical, and biological processes that bring about changes in a sediment subsequent to deposition
204 (Berner, 1980). Phosphorus diagenesis is intimately linked to the diagenesis of iron oxide minerals, as
205 these are the most important carrier phases for reactive phosphorus in sediments (Ruttenberg, 2003).
206 Surface sediments contain both detrital and authigenic forms of oxidized iron, of which the most
207 reactive occur in the authigenic fraction. Iron oxides have been characterized operationally by their
208 reactivity towards hydrogen sulfide (e.g. Canfield, 1989; Roberts, 2015), and various sequential
209 extraction schemes have been designed and applied to distinguish the reactivity of iron oxides towards a
210 variety of reductants (Anschutz et al., 1998; Kostka & Luther, 1994; Poulton & Canfield, 2005;
211 Ruttenberg, 2003). For a recent review of the extensive literature on sequential extraction procedures,
212 we refer to Anschutz & Deborde (2016).

213 Authigenic iron oxides form in the upper part of the sediment column above the depth where the
214 stability boundary for the Fe(II)/Fe(III) redox couple is located. Reactive iron buried below this
215 boundary is reduced to soluble Fe(II) at a rate that depends on the reactivity of Fe(III) phases and
216 organic matter, the availability of which decreases with depth below the sediment surface. Fe(II) is then
217 immobilized as sulfides (in organic-rich sediment) or is transported up by diffusion across the
218 Fe(II)/Fe(III) redox boundary and reoxidized by various oxidants (O_2 , NO_3^- , MnO_2). This “freshly
219 precipitated” iron oxide is reactive and can be recycled multiple times across the Fe(II)/Fe(III) redox
220 boundary before it is finally permanently buried (Canfield et al., 1993). The presence of authigenic iron
221 oxides in the sediment can be quantified according to its reactivity towards a “weak” reductant such as
222 buffered ascorbic acid (Hyacinthe & Van Cappellen, 2004; Kostka & Luther, 1994). Once buried,
223 authigenic iron oxides go through an aging process that includes stepwise dehydration of amorphous
224 phases such as ferrihydrite to goethite and diminishing specific surface area (Lijklema, 1977). This
225 renders reactive iron oxides more refractory, which in addition to diagenetic remobilization is reflected
226 by a diminishing content of ascorbate-extractable iron with depth in the sediment. Thus, the bulk

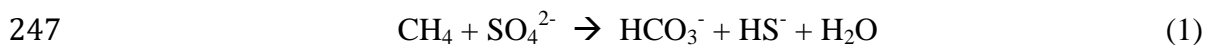
227 reactivity of the sedimentary iron oxides decreases with time (depth of burial). The reactivity of the
228 sedimentary organic matter that survives burial below the oxic surface sediment is also important
229 because the reduction rate of sulfate and production rate of H₂S depend on it. In the section that follows
230 we will introduce methane, a highly mobile form of organic matter that can be oxidized anaerobically in
231 sediments by micro-organisms that use sulfate as terminal electron acceptor.

232

233 ***3.3 Linking phosphorus diagenesis to sea level changes via anaerobic methane oxidation.***

234 Much of our understanding of the early stages of diagenesis rests on the notion that diagenesis is fuelled
235 by the organic carbon that settles to the seafloor and is buried, and that diagenesis comes to an end when
236 this carbon has been fully consumed. However, in continental margin sediments, where immense sub-
237 surface accumulations of methane are present in the form of methane hydrate (e.g., Bohrmann & Torres,
238 2016; Ruppel & Kessler, 2017), methane can support diagenesis above and beyond that fueled by
239 organic matter settling from the water column (Burdige & Komada 2011, 2013; Komada et al., 2016).
240 Methane fuels diagenesis via a number of microbially-mediated processes of which the most important
241 is anaerobic microbial methane oxidation (AOM) using sulfate as terminal electron acceptor (e.g.
242 Boetius et al., 2000; Jørgensen & Kasten, 2006; Nauhaus et al., 2002). AOM has been described as a
243 process that intercepts methane that migrates through anoxic pore water, thereby preventing significant
244 quantities of methane from reaching the atmosphere. However, AOM coupled to sulfate reduction does
245 more than just remove methane; it also produces sulfide and bicarbonate (equation 1).

246



248

249 The sediment layer within which AOM takes place is known as the sulfate methane transition
250 zone (SMT). It can be located at depths varying from centimeters to tens of meters below the sediment
251 surface (Borowski et al., 1999). Riedinger et al. (2014) have made the case for coupled anaerobic
252 oxidation of methane via iron oxide reduction, and Egger et al. (2017) have proposed that a potential
253 coupling between iron oxide reduction and methane oxidation likely affects iron cycling and related
254 biogeochemical processes such as burial of phosphorus. Of special interest here is the production of
255 sulfide, a strong reductant that can reductively dissolve iron oxides and thereby release the associated
256 phosphate into the sediment pore water.

257 At steady state, the SMT would be located at a fixed distance from the sea floor, and the flux of
258 soluble phosphate from the SMT would be controlled by the burial rate of reactive phosphorus.

259 However, the depth of the SMT in continental margin sediments has not necessarily been at steady state
260 on glacial time scales. Meister et al. (2007, 2008) linked diagenetic dolomite formation in hemipelagic
261 sediments to sea level changes, showing that the SMT migrates upwards and downwards within the
262 sediment column. They hypothesized that the SMT persists within an organic carbon-rich interglacial
263 sediment layer sandwiched between layers of organic carbon-poor glacial sediment. Contreras et al.
264 (2013) reported evidence showing that the SMT in organic carbon-rich sediments from the highly
265 productive Peruvian shelf was located at much shallower burial depths than the present SMT.

266 The location of the SMT in the sediment column is critical since this is where the reduction of
267 iron oxides releases phosphate to the pore water. The closer the SMT is to the sediment surface, the
268 greater is the flux of sulfate into the sediment and the shorter is the path that phosphate travels before it
269 escapes the sediment. The upward displacement of the SMT and the instantaneous flux of phosphate to
270 the ocean can be linked to the rate of sea-level fall if we assume that a time-variable supply of methane
271 from methane hydrate-bearing sediment layers can also bring about a fluctuating SMT.

272

273 ***3.4 Background (steady - state) fluxes of methane and phosphate in methane hydrate bearing***
274 ***sediment.*** The depth distribution of methane hydrate in sediments is constrained by the relatively narrow
275 pressure and temperature range within which methane hydrate is stable and can exist as a solid (e.g.,
276 Ruppel & Kessler, 2017). The lower and upper boundaries of the methane hydrate stability field respond
277 to the accumulation and burial of successive layers of fresh sediment by migrating upward towards the
278 seafloor. Methane hydrate located at the lower stability boundary is thereby transported below this
279 boundary, where it becomes unstable, dissociates, and releases methane into the pore water.
280 Consequently, the downward directed burial flux of sediment is accompanied by an upward directed flux
281 of methane.

282 The lower stability boundary for methane hydrate can be observed seismically as a discontinuity
283 in sound transmission as a gas-rich layer develops. Recent high-resolution seismic data from the Blake
284 Ridge crest (Borowski et al. 1999) show that methane gas, produced by hydrate dissociation at the lower
285 stability boundary, can be injected well into the overlying hydrate stability zone. The data indicate that
286 methane, in the form of free gas, can migrate hundreds of meters into the hydrate stability zone before
287 re-forming as solid phase hydrate (Gorman et al., 2002). The ability of gaseous methane to migrate
288 across a thermodynamic regime where it should be trapped as a hydrate suggests that gas migration
289 through the sediment column plays an important role in the interaction of sub-seafloor methane with the
290 overlying ocean. Under steady state conditions, the upper boundary of the methane hydrate stability field

291 would keep pace with the rate of sediment accumulation, which would create a zone in the upper
292 sediment column within which methane can be removed from the pore water by solid phase hydrate
293 precipitation. In the presence of sulfate, which is in abundant supply in the overlying ocean, methane can
294 also be removed from the pore water by anaerobic methane oxidation. According to the stoichiometry of
295 AOM (Equation 1), the upward flux of methane into the SMT should equal the downward flux of sulfate.
296 In the absence of electron donors other than methane, a linear pore-water sulfate gradient is expected
297 and can be used to estimate the instantaneous methane flux (Borowski et al., 1999).

298 **3.5 Sea-level changes and methane and phosphate fluxes in the sediment.** Because of the
299 sensitivity of methane hydrate deposits to changes in temperature and pressure, one can expect that
300 fluctuations in sea level and temperature, both of which are associated with glacial cycles, will perturb
301 the depth distribution of methane in the sediment. For example, the hydrostatic pressure decrease that
302 was associated with the 120 m sea-level drop during the last glacial maximum has been estimated to
303 lower the hydrostatic pressure enough to raise the lower boundary of the gas hydrate stability field by as
304 much as 20 m (Dillon & Max, 1983). There can therefore be little doubt that a perturbation such as a
305 sea-level drop can cause methane to be released into the pore water and thereby increase the
306 instantaneous fluxes of methane and phosphate above and beyond the slower background fluxes
307 sustained by steady-state sediment accumulation (section 3.4).

308 The stoichiometry of anaerobic methane oxidation requires that the flux of sulfate into the
309 sediment must increase in order to accommodate an increased upward flux of methane (Equation 1).
310 This implies that the sulfate gradient grows steeper and that the SMT migrates upward. As the SMT
311 moves upward, so does the Fe(II)/Fe(III) redox boundary, expanding the pool of iron oxides that is
312 exposed to reducing conditions. An upward directed migration of the SMT and the expansion of the pool
313 of oxidized Fe can also be expected to increase the abundance of dissolved ferrous iron and generate a
314 downward directed flux of Fe(II) into the sediment region located below the SMT. It has been suggested
315 (März et al. 2018) that this might be one of the conditions (among others) that would lead to autigenesis
316 of Fe(II) minerals, such as vivianite.

317 The location of the SMT is important because the closer it is to the sediment surface the steeper
318 will be the phosphate gradient that drives phosphate towards and across the sediment-water interface.
319 Recent syntheses of global sea-level records (Foster & Rohling, 2013; Lambec et al., 2014; Wallmann et
320 al., 2016) show that there were several episodes of sea-level fall during the last glaciation, each episode
321 interrupted by periods of stable sea level. This suggests that there could also have been several pulses of

322 methane release into the pore water, which would cause the sub-bottom depth of the SMT and the
323 reactions associated with it to fluctuate.

324 The phosphate flux cannot be expected to mirror directly the fluxes of methane and sulfate
325 because the reductive dissolution rate of the sedimentary iron oxide pool is not constant but depends on
326 the reactivity of the individual iron oxides present in the sediment (Canfield, 1989). Furthermore, the
327 efflux of phosphate is ultimately limited by the pool of reactive phosphorus that is present in the
328 sediment column when sea-level falls.

329

330 **3.6 Transport of phosphate in sediment pore waters: adsorption and desorption.** Relative to the
331 sediment surface, burial moves reactive particulate phosphorus downward into the sediment column
332 while diffusion moves soluble phosphate upwards. The two oppositely directed phosphorus fluxes
333 interact by partitioning soluble phosphate between solution and sorption sites on solid surfaces, mostly
334 to iron oxides (e.g. Krom and Berner, 1980, 1981; Sundby et al., 1992). Phosphate also adsorbs onto
335 other solids, including Mn-oxides and carbonate minerals (Millero et al., 2001; Yao and Millero, 1996).
336 It can also form authigenic carbonate fluorapatite (März et al., 2018). It has been observed that all the
337 iron oxide surfaces found in oxic continental margin sediments are “saturated” with phosphate (all
338 available sorption sites are occupied) and that the detrital iron oxide fraction is already saturated in
339 phosphate by the time it arrives on the sea floor (Anschutz and Chaillou, 2009). Irrespective, sorption
340 sites soon become saturated upon burial below the sediment-water interface where organic phosphorus is
341 rapidly remineralized and pore-water phosphate reaches saturation levels (Sundby et al., 1992). Sorption
342 should therefore not restrict the transport of phosphate diffusing up from the SMT towards the sea floor.

343 Evidence that phosphate can be transported over large depth intervals in sediments without the
344 pore-water profile being visibly affected by sorption onto sediment particles can be found in the data set
345 of Niewohner et al. (1998). Four 12-15 m long cores collected in 1300-2000 m water depth from gas
346 hydrate-bearing sediments on the continental margin off Namibia display linear pore-water phosphate
347 profiles. In two of the cores, the phosphate profile is linear over a 15 m depth interval, from the
348 sediment-water interface to the bottom of the cores; the two other cores display a slope change at about
349 2 m depth, below which the profile is linear. We do not wish to imply that these profiles are
350 representative of glacial sediments, but they do illustrate an important point: It is possible for phosphate
351 to diffuse over long distances in sediment pore water without encountering significant impediment by
352 secondary diagenetic reactions.

353

354 4. LINKING THE PHOSPHORUS CYCLE TO CHANGES IN ATMOSPHERIC CO₂

355

356 **4.1. The concept of a limiting nutrient.** A nutrient is limiting if its addition to the system
357 increases the rate of net primary production. Because phosphorus and nitrogen both are essential
358 elements for life, there has been much debate about which of these elements limits photosynthetic
359 primary production in the ocean (e.g. Falkowski, 1997; Galbraith et al., 2008; Lenton & Watson, 2000;
360 Smith, 1984; Tyrrell, 1999). Oceanic inventories of nitrogen have undergone large changes between
361 glacial and interglacial periods (Ganeshram et al., 1995, 2002), which has been attributed to greatly
362 diminished water column denitrification and consequent increase in the nitrate inventory during glacial
363 periods. In the modern ocean, it appears that nitrogen is the limiting nutrient. Therefore, increasing the
364 flux of phosphate into the ocean would not necessarily increase the rate of primary production.
365 Nevertheless, irrespective of which nutrient element is limiting, primary production assimilates
366 phosphate into biomass, which settles to the sea floor and is buried under successive layers of new
367 sediment. In this way, phosphorus is transferred from the oceanic reservoir to the sedimentary reservoir.
368 Likewise, the net result of methane-fuelled diagenesis is to return phosphate, a nutrient element, from
369 the sedimentary to the oceanic phosphorus reservoir.

370

371 **4.2. Expansion and contraction of phosphorus reservoirs during a glacial cycle.** The central
372 idea of the simple two-reservoir representation of the phosphorus cycle proposed by Broecker (1982a,
373 1982b) is that the phosphorus inventory in a reservoir can contract and expand on glacial time scales,
374 eventually impacting the CO₂ level in the atmosphere. This simple representation of otherwise complex
375 phenomena has stimulated research on the mechanism that control nutrient fluxes in the ocean.

376 Boyle (1986) showed that the oceanic phosphorus inventory can vary on a glacial time scale. He
377 concluded, based on the cadmium content of foraminifera and carbon isotope measurements, that the
378 phosphate content of the ocean during the last glacial maximum was 17% larger than it is at present.
379 Likewise, Wallmann (2010) found that the pre-human modern ocean was losing dissolved phosphate (to
380 the sedimentary P-reservoir) at a rate of about 5% Kyr⁻¹. The 'lost' phosphate is assimilated into
381 biomass and/or adsorbed onto mineral particles, the settling of which returns reactive phosphorus to the
382 sediment. Colman & Holland (2000), who examined phosphate cycling in modern continental margin
383 sediments, concluded that the current efflux of phosphate from continental margin sediments is about
384 one half of the total settling flux of particulate reactive phosphorus. The portion that settles through the

385 ocean water column to the sea floor is eventually converted to stable minerals and lost from the oceanic
386 phosphorus cycle.

387 **4.3. Chronology of events during a glacial phosphorus cycle.** With the initiation of a glacial
388 cycle, the global temperature decreases, ice builds up on the continents, the sea level falls, the pressure
389 on the sea floor decreases, and the upper and lower boundaries of the methane hydrate stability field in
390 the sediment column shift upward. Methane hydrate located below the lower stability boundary becomes
391 unstable and decomposes. Methane gas is released to the pore water, the concentration gradient becomes
392 steeper, and the upward methane flux increases. Upward migrating methane encounters downward
393 diffusing sulfate in the sulfate-methane transition zone (SMT). Here, methane is oxidized to CO₂ and
394 sulfate is reduced to sulfide (Eqn. 1). The reaction between sulfide and oxidized Fe-species reduces
395 Fe(III) to Fe(II), and phosphate associated with oxidized Fe is released into the pore waters, increasing
396 the phosphorus flux into the oceanic reservoir. Irrespective of which nutrient is limiting, primary
397 production in the photic zone assimilates nutrients into biomass, lowering the inventory and
398 concentration of reactive phosphorus and other nutrients in the oceanic reservoir. The fraction of
399 reactive phosphorus that becomes buried on the continental margin is not necessarily lost to the marine
400 phosphorus cycle. It may conceivably become remobilized by diagenesis during an eventual new glacial
401 cycle.

402 During times when the sea level remains stable, and assuming that sediment accumulation and
403 burial still take place, methane fuelled diagenesis can nevertheless occur. This is because the migration
404 of the upper and lower boundaries of the methane hydrate stability field tracks the burial of sediment.
405 When this happens, gas hydrates previously located within the hydrate stability field—and thus stable—
406 become exposed to destabilizing conditions and release methane, and subsequently phosphate, to the
407 pore water. A flux of phosphate—what we call a ‘background’ flux— can therefore be delivered to the
408 ocean even when the sea level remains stable. When sea level change is then superimposed, the net
409 result is to amplify the phosphate flux to the ocean beyond the background flux.

410 Sea level driven diagenetic transfer of phosphate from sediment to ocean continues throughout
411 the glaciation period, perhaps in spurts because of intervals of stable sea level. When, finally, after the
412 deglaciation, when sea level and pressure on the seafloor have reached stable values, diagenetically
413 driven fluxes from the sediment stabilize on pre-glaciation background values. Towards the end of the
414 glaciation period, the stratification of the water column destabilizes (e.g., Basak et al., 2008), which
415 facilitates vertical mixing and brings CO₂-rich deep water to the photic zone. The biological pump
416 having been weakened by the ongoing biological removal of soluble reactive phosphorus from the

417 oceanic reservoir and the physical pump having gained strength, transport of nutrient-poor / CO₂-rich
418 water to the surface ocean will favour the escape (outgassing) of CO₂ into the atmosphere.

419

420 **4.4. The timing of the exchange of phosphorus between ocean and sediment.** The key to
421 understanding the glacial phosphorus cycle lies in the timing of the transformation of phosphorus from
422 one form to another and the transfer from one phosphorus-reservoir to the other. Under the two-reservoir
423 methane-fuelled diagenetic scenario, the transfer of phosphate from the sedimentary reservoir to the
424 oceanic reservoir begins when the sea-level falls. The initial phosphate release from the sedimentary
425 reservoir would likely be a pulse because, occurring at the end of a long time (nearly a complete glacial
426 cycle) of transfer of reactive phosphorus to the sedimentary reservoir, this is when the sedimentary
427 phosphorus inventory would be at a maximum.

428 The scenarios that have been proposed to explain variations of the CO₂ concentration in the
429 atmosphere fall into two groups. A biological pump relies on photosynthesis to convert CO₂ to biomass,
430 thereby lowering the partial pressure of CO₂ in the surface ocean. A physical pump relies on the vast
431 quantity of CO₂ sequestered in the deep ocean that can be brought to the surface ocean by vertical
432 mixing and advection. The net effect of each type of pump—draw-down from the atmosphere or
433 outgassing into the atmosphere— depends on the resulting partial CO₂ pressure gradient across the air-
434 sea interface (e.g., Hain et al., 2014). The ice-core record of atmospheric CO₂ (Petit et al., 1999; Sigman
435 & Boyle, 2000) shows that, during glacial periods, the atmospheric CO₂ concentration decreased
436 gradually from values as high as 280-300 ppm near the beginning of a glaciation to less than 200 ppm at
437 the end. The decrease in atmospheric CO₂ typically took place over about 90,000 years, and was similar
438 for each of the previous three glaciation cycles. The average rate at which atmospheric CO₂ *decreased*
439 throughout the last glacial period was roughly 1 ppm Kyr⁻¹. This is slower than the rate at which
440 atmospheric CO₂ *increased* during the transition from the glacial period to the interglacial period that
441 preceded it (Sowers and Bender, 1995). Ice-core data also show that the atmospheric CO₂ level peaked
442 rapidly during the termination of each glacial period. The methane-driven phosphorus scenario predicts
443 that phosphate is transferred to the ocean from the sedimentary phosphorus reservoir during the early
444 stages of a glacial cycle, after the sea level has begun to fall.

445 The concentration of CO₂ sequestered in the deep (> 1000m) waters of the oceanic reservoir is
446 higher than in the surface ocean reservoir because a fraction of the organic matter produced in the
447 surface ocean settles towards the deep seafloor and is remineralized by microbial processes. The deep
448 ocean contains nearly ten times more carbon than the atmosphere, surface-ocean, and terrestrial systems
449 combined, and the pCO₂ of the deep-ocean water is well buffered on long time scales via reactions of
450 the carbonate system, including the dissolution of biogenic carbonates. The dissolved inorganic carbon
451 inventory in the deep ocean does not, therefore, respond rapidly to changes in the sinking flux of
452 mineralizable organic matter, but remains high. Deep water is exposed at the ocean surface roughly
453 every 1,000 years or 100 times during a complete glacial cycle (Broecker & Peng, 1982; DeVries &
454 Primeau, 2011; Sigman & Boyle, 2000), which attenuates CO₂ changes on the time scale of glaciations.

455

456 **5. SUMMARY AND CONCLUSIONS**

457

458 We have modified the two-reservoir scenario of the marine phosphorus cycle proposed by
459 Broecker (1982a, 1982b) to include a diagenetic mechanism that allows for phosphorus to be exchanged
460 between the sedimentary and the oceanic phosphorus reservoirs on glacial time scales. Within the
461 scenario a coupled series of processes acts upon the glacial – interglacial marine phosphorus cycle (table
462 1).

463 During a glaciation period, water is transferred from the ocean to continental ice sheets. The
464 falling sea level lowers the hydrostatic pressure on the seafloor. The pressure change perturbs the
465 stability field of methane hydrates, and methane gas is released into the pore water. The release of
466 methane gas from gas hydrates amplifies the upward flux of methane through the sediment column. In
467 the sulfate-methane-transition zone (SMT), where methane is removed via anaerobic methane oxidation,
468 the increased methane supply increases the demand for sulfate. The sulfate gradient steepens, and the
469 SMT zone moves closer to the sediment-water interface. Reactions within the SMT produce hydrogen
470 sulfide, which reductively dissolves iron oxides. Iron-bound phosphate can then be released into the pore
471 water. The upward directed phosphate gradient steepens, which increases the flux of phosphate towards
472 and across the sediment-water interface and increases the phosphate inventory of the ocean.

473 Phosphorus is transferred from the oceanic to the sedimentary reservoir by sedimentation and
474 burial of phosphorus-containing biogenic particulate matter resulting from primary production and
475 abiotic particulate matter on which phosphate is adsorbed. Unlike the release of phosphate from the

476 sediment, the return flux of phosphorus to the sediment and the associated depletion of the oceanic
477 reactive phosphorus inventory do not occur as an event but take place throughout the glacial cycle.
478 Burial of organic matter causes a corresponding loss of phosphorus from the oceanic inventory. If
479 phosphorus were the nutrient limiting primary production at the time leading up to the release, primary
480 production would be stimulated by the added phosphate to the surface ocean, CO₂ would be drawn down
481 from the atmosphere, and the phosphorus inventory would begin to decrease. If, on the other hand,
482 nitrogen nutrients were to become limiting, which is likely when new phosphate is added to the surface
483 ocean reservoir, the rates of primary production, phosphorus burial, and draw-down of atmospheric CO₂
484 would slow down until the fixed nitrogen to phosphorus ratio became similar to the Redfield ratio. It is
485 therefore not unreasonable to expect that with a gradual depletion of phosphorus in the ocean, a stable
486 N:P ratio would develop, co-limiting primary production in the ocean (e.g., Lenton & Watson, 2000;
487 Lenton & Klausmeier, 2007). As the glaciation progresses, the ocean will gradually become nutrient
488 depleted irrespective of which is the limiting nutrient. This would weaken the biological pump relative
489 to the physical pump (upwelling of deep CO₂-rich water) and set the stage for a tipping point beyond
490 which atmospheric CO₂ is controlled by upwelling of CO₂-rich deep water. The next glaciation period,
491 which is accompanied by sea-level fall, methane-hydrate decomposition, anaerobic methane oxidation,
492 and phosphate release allows the biological pump to once again take control over atmospheric CO₂.

493 Inventories of reactive particulate phosphorus in the ocean and in continental margin sediments
494 can change on glacial-interglacial time scales as phosphorus is transferred from the sediment column to
495 the water column and *vice versa*. Responding to a fall in sea level, phosphorus is transferred from the
496 sediment to the ocean. This involves destabilization of methane hydrate, an increase of the methane flux
497 through the sediment column, and an increase in the rate of anaerobic methane oxidation. The elevated
498 methane flux drives an increasing demand for sulfate and consequent production of sulfide. Sulfide
499 reduces sedimentary iron oxides and releases associated phosphate to the pore water through which it
500 can migrate across the sediment-water interface and increase the surface ocean inventory of phosphorus.
501 Since sea level fall may not occur as a single event but may include stable periods, phosphate release
502 may likewise occur episodically. The latter would depend on the extent to which the phosphate
503 contained in the sedimentary reservoir has been depleted and on the amount of time available to
504 recharge the sedimentary reservoir between sea-level change events. The link between sea level fall, gas
505 hydrate destabilization and the upward migration of the sulfate-methane-transition zone establishes the
506 timing of phosphate releases to the surface ocean reservoir during the glaciation period, likely during the
507 initial episode of sea level fall.

508 The proposed scenario capitalizes on elements of Broecker's model and provides another
509 potential trigger to the suite of processes that may have contributed to the rapid glacial-interglacial
510 climate transitions documented in paleo-records.

511

512 **ACKNOWLEDGEMENTS**

513 No new data are presented in this manuscript, which is inspired by and developed with data in
514 the public domain. These are cited in the references included in the manuscript. B.S. and A.M. gratefully
515 acknowledge the financial support from the Natural Sciences and Engineering Research Council of
516 Canada through their Discovery grants.

517

518 **REFERENCES**

- 519 Anschutz, P. & Chaillou, G. (2009). Deposition and fate of reactive Fe, Mn, P, and C in suspended particulate matter in
520 the Bay of Biscay. *Continental Shelf Research*, 29(8), 1038-1043.
- 521 Anschutz, P. & Deborde, J. (2016). Spectrophotometric determination of phosphate in matrices from sequential
522 leaching of sediments. *Limnology and Oceanography: Methods*, 14(4), 245-256.
- 523 Anschutz, P., Zhong, S., Sundby, B., Mucci, A. & Gobeil, C. (1998). Burial efficiency of phosphorus and the geochemistry
524 of iron in continental margin sediments. *Limnology and Oceanography*, 43(1), 53-64.
- 525 Archer, D. (2007). Methane hydrate stability and anthropogenic climate change. *Biogeosciences Discussions*, 4(2),
526 993-1057.
- 527 Archer, D., Winguth, A., Lea, D. & Mahowald, N. (2000). What caused the glacial/interglacial atmospheric pCO₂ cycles?
528 *Reviews of Geophysics*, 38(2), 159-189.
- 529 Barnola, J.M., Raynaud, D.Y.S.N., Korotkevich, Y.S. & Lorius, C. (1987). Vostok ice core provides 160,000-year record of
530 atmospheric CO₂. *Nature*, 329(6138), 408-414.
- 531 Basak C., Fröllje, H., Lamy, F., Gersonde, R. Benz, V. Anderson R. F. et al. (2018). Breakup of last glacial deep
532 stratification in the South Pacific. *Science*, 359, 900-904.
- 533 Berner, R.A. (1980). *Early Diagenesis: A Theoretical Approach*, Princeton University Press.
- 534 Berner, R.A., Ruttenberg, K.C., Ingall, E.D. & Rao, J.L. (1993). The nature of phosphorus burial in modern marine
535 sediments. In R. Wollast, F. T. Mackenzie & L. Chou (eds) *Interactions of C, N, P and S biogeochemical cycles and global*
536 *change* (pp. 365-378). Springer, Berlin, Heidelberg.
- 537 Boetius, A., Ravenschlag, K., Schubert, C.J., Rickert, D., Widdel, F., Gieseke, A., et al. (2000). A marine microbial
538 consortium apparently mediating anaerobic oxidation of methane. *Nature*, 407(6804), 623-626.
- 539 Bohrmann G. & Torres M.E. (2006). Gas hydrates in marine sediments. In H. D. Schulz & M. Zabel (eds.) *Marine*
540 *Geochemistry*. (pp. 481-512) Springer, Berlin, Heidelberg.

- 541 Borowski, W.S., Paull, C.K. & Ussler, W. (1999). Global and local variations of interstitial sulfate gradients in deep-
542 water, continental margin sediments: Sensitivity to underlying methane and gas hydrates. *Marine Geology*, 159(1-4),
543 131-154.
- 544 Boyle, E.A. (1986). Paired carbon isotope and cadmium data from benthic foraminifera: Implications for changes in
545 oceanic phosphorus, oceanic circulation, and atmospheric carbon dioxide. *Geochimica et Cosmochimica Acta*, 50(2),
546 265-276.
- 547 Broecker, W.S., (1982a). Glacial to interglacial changes in ocean chemistry. *Progress in Oceanography*, 11(2), 151-197.
- 548 Broecker, W.S. (1982b). Ocean chemistry during glacial time. *Geochimica et Cosmochimica Acta*, 46(10), 1689-1705.
- 549 Broecker, W.S. (2018). Glacial Cycles. *Geochemical Perspectives*, 7(2), 167-181.
- 550 Broecker, W.S. & Peng, T.H. (1982). *Tracers in the Sea*. Eldigio Press, New York, 1-690
- 551 Burdige, D.J. & Komada, T. (2011). Anaerobic oxidation of methane and the stoichiometry of remineralization
552 processes in continental margin sediments. *Limnology and Oceanography*, 56(5), 1781-1796.
- 553 Burdige, D.J. & Komada, T. (2013). Using ammonium pore water profiles to assess stoichiometry of deep
554 remineralization processes in methanogenic continental margin sediments. *Geochemistry, Geophysics, Geosystems*,
555 14(5), 1626-1643.
- 556 Canfield, D. E. (1989). Reactive iron in marine sediments. *Geochimica et Cosmochimica Acta*, 53, 619-632
- 557 Canfield, D.E., Thamdrup, B. & Hansen, J.W. (1993). The anaerobic degradation of organic matter in Danish coastal
558 sediments: iron reduction, manganese reduction, and sulfate reduction. *Geochimica et Cosmochimica Acta*, 57(16),
559 3867-3883.
- 560 Cartapanis, O., Bianchi, D., Jaccard, S.L. and Galbraith, E.D., 2016. Global pulses of organic
561 carbon burial in deep-sea sediments during glacial maxima. *Nature communications*, 7(1),
562 pp.1-7.
- 563 Colman, A.S. & Holland, H.D. (2000). The global diagenetic flux of phosphorus from marine sediments to the oceans:
564 redox sensitivity and the control of atmospheric oxygen levels. *SEPM Special Publication No. 66*. 53-75.
565 doi.org/10.2110/pec.00.66.0053
- 566 Contreras, S., Meister, P., Liu, B., Prieto-Mollar, X., Hinrichs, K.U., Khalili, A., et al. (2013). Cyclic 100-ka (glacial-
567 interglacial) migration of subseafloor redox zonation on the Peruvian shelf. *Proceedings of the National Academy of*
568 *Sciences*, 110(45), 18098-18103.
- 569 Delaney M. (1998). Phosphorus accumulation in marine sediments and the oceanic phosphorus cycle. *Global*
570 *Biogeochemical Cycles*, 12, 563-572.
- 571 DeVries, T. & Primeau, F. (2011). Dynamically and observationally constrained estimates of water-mass distributions
572 and ages in the global ocean. *Journal of Physical Oceanography*, 41(12), 2381-2401.
- 573 Dillon, W.P. & Max, M.D. (2000). Oceanic Gas Hydrate. In M.D. Max (ed.) *Natural Gas Hydrate in Oceanic and*
574 *Permafrost Environments* (pp. 61-76), Dordrech, NL: Kluwer.
- 575 Egger M., Hagens M., Sapart C. J., Dijkstra N., van Helmond N. A. G. M., Mogollón J. M., et al. (2017). Iron oxide reduction
576 in methane-rich deep Baltic Sea sediments. *Geochimica et Cosmochimica Acta*, 207, 256-276.

- 577 Egger, M., Jilbert, T., Behrends, T., Rivard, C. & Slomp, C.P. (2015) Vivianite is a major sink for phosphorus in
578 methanogenic coastal surface sediments. *Geochimica et Cosmochimica Acta*, 169, 217–235.
- 579 Egger, M., Kraal, P., Jilbert, T., Sulu-Gambari, F., Sapart, C. J., Röckmann, T. & Slomp, C. P. (2016) Anaerobic oxidation of
580 methane alters sediment records of sulfur, iron and phosphorus in the Black Sea, *Biogeosciences*, 13, 5333–5355.
- 581 Falkowski, P.G. (1997). Evolution of the nitrogen cycle and its influence on the biological sequestration of CO₂ in the
582 ocean. *Nature*, 387(6630), 272-275.
- 583 Filippelli, G.M. (1997). Controls on phosphorus concentration and accumulation in oceanic sediments. *Marine Geology*,
584 139(1-4), 231-240.
- 585 Foster, G.L. & Rohling, E.J. (2013). Relationship between sea level and climate forcing by CO₂ on geological timescales.
586 *Proceedings of the National Academy of Sciences*, 110(4), 1209-1214.
- 587 Galbraith, E. D, Sigman, D., Pedersen, T. & Robinson, R. S. (2008). Past changes in the marine nitrogen cycle. In D.
588 Capone, D. Bronk, M. Mulholland & E. Carpenter (eds.) *Nitrogen in the Marine Environment*, 2nd edition (pp. 1497-
589 1535), Elsevier. doi 10.1016/B978-0-12-372522-6.00034-7.
- 590 Ganeshram, R.S., Pedersen, T.F., Calvert, S. & François, R. (2002). Reduced nitrogen fixation in the glacial ocean
591 inferred from changes in marine nitrogen and phosphorus inventories. *Nature*, 415(6868), 156-159.
- 592 Ganeshram, R.S., Pedersen, T.F., Calvert, S.E. & Murray, J.W. (1995). Large changes in oceanic nutrient inventories from
593 glacial to interglacial periods. *Nature*, 376(6543), 755-758.
- 594 Gorman, A.R., Holbrook, W.S., Hornbach, M.J., Hackwith, K.L., Lizarralde, D. & Pecher, I. (2002). Migration of methane
595 gas through the hydrate stability zone in a low-flux hydrate province. *Geology*, 30(4), .327-330.
- 596 Hain, M.P., Sigman, D.M. & Haug, G.H. (2014). The biological Pump in the Past. *Treatise on Geochemistry (Second*
597 *Edition)*, *The Oceans and Marine Geochemistry*, 8, 485-517.
- 598 Hsu, T. W., Jiang, W. T. & Wang, Y. (2014) Authigenesis of vivianite as influenced by methane-induced sulfidization in
599 cold-seep sediments off southwestern Taiwan. *Journal of Asian Earth Sciences*. 89, 88–97.
- 600 Hyacinthe, C. & Van Cappellen, P. (2004). An authigenic iron phosphate phase in estuarine sediments: composition,
601 formation and chemical reactivity. *Marine Chemistry*, 91(1-4), 227-251.
- 602 Jørgensen, B.B. & Kasten, S. (2006). Sulfur cycling and methane oxidation. In H. D. Schulz & M. Zabel (eds.), *Marine*
603 *Geochemistry* (pp. 271-302). Springer,
- 604 Kohfeld, K.E., Le Quéré, C., Harrison, S.P. & Anderson, R.F. (2005). Role of marine biology in glacial-interglacial CO₂
605 cycles. *Science*, 308(5718), 74-78.
- 606 Komada, T., Burdige, D.J., Li, H.L., Magen, C., Chanton, J.P. & Cada, A.K. (2016). Organic matter cycling across the sulfate-
607 methane transition zone of the Santa Barbara Basin, California Borderland. *Geochimica et Cosmochimica Acta*, 176,
608 259-278.
- 609 Kostka, J.E. & Luther III, G.W. (1994). Partitioning and speciation of solid phase iron in saltmarsh sediments.
610 *Geochimica et Cosmochimica Acta*, 58(7), 1701-1710.
- 611 Krom M. D. & Berner, R. A. (1981). The diagenesis of phosphorus in a nearshore marine sediment. *Geochimica et*
612 *Cosmochimica Acta*, 45(2), 207-216.

- 613 Krom, M.D. & Berner, R.A. (1980). The diffusion coefficients of sulfate, ammonium, and phosphate ions in anoxic
614 marine sediments. *Limnology and Oceanography*, 25, 327-337.
- 615 Kvenvolden, K.A. (1993). Gas hydrates – Geological perspective and global change. *Reviews of Geophysics*, 31(2), 173-
616 187.
- 617 Lambeck, K., Rouby, H., Purcell, A., Sun, Y. & Sambridge, M. (2014). Sea level and global ice volumes from the Last
618 Glacial Maximum to the Holocene. *Proceedings of the National Academy of Sciences*, 111(43), 15296-15303.
619 Lenton, T.M. & Klausmeier, C.A. (2007). Biotic stoichiometric controls on the deep ocean N: P ratio. *Biogeosciences*, 4, 353-
620 367.
- 621 Lenton, T.M. & Watson, A.J. (2000). Redfield revisited: 1. Regulation of nitrate, phosphate, and oxygen in the ocean.
622 *Global Biogeochemical Cycles*, 14(1), 225-248.
- 623 Lijklema, L. (1977). The role of iron in the exchange of phosphate between water and sediments. In: H. L. Golterman
624 (ed.), *Interactions Between Sediments and Fresh Water*. (pp. 313-317) Dr W. Junk Publishers, The Hague.
- 625 Liu, J., Izon, G., Wang, J., Antler, G., Wang, Z. & Egger, M. (2018) Vivianite formation in methane-rich deep-sea
626 sediments from the South China Sea. *Biogeosciences*, 15, 6329-6348.
- 627 März, C., Hoffmann, J., Bleil, U., De Lange, G. & Kasten, S. (2008) Diagenetic changes of magnetic and geochemical
628 signals by anaerobic methane oxidation in sediments of the Zambezi deep-sea fan (SW Indian Ocean). *Marine Geology*,
629 255, 118–130.
- 630 März, C., Riedinger, N., Sena, C. & Kasten, S. (2018). Phosphorus dynamics around the sulphate-methane transition in
631 continental margin sediments: Authigenic apatite and Fe (II) phosphates. *Marine Geology*, 404, 84-96.
- 632 Meister, P., Bernasconi, S.M., Vasconcelos, C. & McKenzie, J.A. (2008). Sea level changes control diagenetic dolomite
633 formation in hemipelagic sediments of the Peru Margin. *Marine Geology*, 252(3-4), pp.166-173.
- 634 Meister, P., McKenzie, J.A., Vasconcelos, C., Bernasconi, S., Frank, M., Gutjahr, M. & Schrag, D.P. (2007). Dolomite
635 formation in the dynamic deep biosphere: results from the Peru Margin. *Sedimentology*, 54(5), 1007-1032.
- 636 Millero F.J., Huang F., Zhu X. & Zhang J.-Z. (2001). Adsorption and desorption of phosphate on calcite and aragonite in
637 seawater. *Aquatic Geochemistry*, 7(1), 33-56.
- 638 Nauhaus, K., Boetius, A., Krüger, M. & Widdel, F. (2002). In vitro demonstration of anaerobic oxidation of methane
639 coupled to sulphate reduction in sediment from a marine gas hydrate area. *Environmental Microbiology*, 4(5), 296-
640 305.
- 641 Niewöhner, C., Hensen, C., Kasten, S., Zabel, M. & Schulz, H.D. (1998). Deep sulfate reduction completely mediated by
642 anaerobic methane oxidation in sediments of the upwelling area off Namibia. *Geochimica et Cosmochimica Acta*,
643 62(3), 455-464.
- 644 Paull, C.K., Brewer, P.G., Ussler, W., Peltzer, E.T., Rehder, G. & Clague, D. (2002). An experiment demonstrating that
645 marine slumping is a mechanism to transfer methane from seafloor gas-hydrate deposits into the upper ocean and
646 atmosphere. *Geo-Marine Letters*, 22(4), 198-203.
- 647 Paull, C.K., Ussler, W. & Dillon, W.P. (1991). Is the extent of glaciation limited by marine gas hydrates? *Geophysical*
648 *Research Letters*, 18(3), 432-434.
- 649 Peacock, S., Lane, E. & Restrepo, J.M. (2006). A possible sequence of events for the generalized glacial-interglacial
650 cycle. *Global Biogeochemical Cycles*, 20, GB2010. doi.org/10.1029/2005GB002448

- 651 Petit, J.R., Jouzel, J., Raynaud, D., Barkov, N.I., Barnola, J.M., Basile, I., et al. (1999). Climate and atmospheric history of
652 the past 420,000 years from the Vostok ice core, Antarctica. *Nature*, 399(6735), 429-436
- 653 Poulton, S.W. & Canfield, D.E. (2005). Development of a sequential extraction procedure for iron: implications for iron
654 partitioning in continentally derived particulates. *Chemical Geology*, 214(3-4), 209-221.
- 655 Riedinger, N., Formolo, M.J., Lyons, T.W., Henkel, S., Beck, A. & Kasten, S. (2014). An inorganic geochemical argument
656 for coupled anaerobic oxidation of methane and iron reduction in marine sediments. *Geobiology*, 12(2), 172-181.
- 657 Roberts, A.P. (2015). Magnetic mineral diagenesis. *Earth-Science Reviews*, 151, 1-47.
- 658 Rothe, M., Kleeberg, A. & Hupfer, M. (2016) The occurrence, identification and environmental relevance of vivianite in
659 waterlogged soils and aquatic sediments. *Earth-Science Review*, 158, 51-64.
- 660 Ruppel, C.D. & Kessler, J.D. (2017). The interaction of climate change and methane hydrates. *Reviews of Geophysics*,
661 55(1), 126-168.
- 662 Ruttenger, K.C. (2003). The global phosphorus cycle. In: W.H. Schlesinger (ed.), *Treatise on Geochemistry*, Vol. 8, pp.
663 585-643.
- 664 Siddall, M., Rohling, E.J., Almogi-Labin, A., Hemleben, C., Meischner, D., Schmelzer, I. & Smeed, D.A. (2003). Sea level
665 fluctuations during the last glacial cycle. *Nature*, 423(6942), 853-858.
- 666 Sigman, D.M. & Boyle, E.A. (2000). Glacial/interglacial variations in atmospheric carbon dioxide. *Nature*, 407(6806),
667 859-869.
- 668 Sigman, D.M., Hain, M.P. & Haug, G.H. (2010). The polar ocean and glacial cycles in atmospheric CO₂ concentration.
669 *Nature*, 466(7302), 47-55.
- 670 Slomp, C. P., Mort, H. P., Jilbert, T., Reed, D. C., Gustafsson, B. G. & Wolthers, M. (2013) Coupled dynamics of iron and
671 phosphorus in sediments of an oligotrophic coastal basin and the impact of anaerobic oxidation of methane, *PloS one*,
672 8, e62386
- 673 Smith, S.V. (1984). Phosphorus versus nitrogen limitation in the marine environment. *Limnology and Oceanography*,
674 29(6), 1149-1160.
- 675 Sowers, T. & Bender, M. (1995). Climate records covering the last deglaciation. *Science*, 269(5221), 210-214.
- 676 Sundby B., Gobeil C., Silverberg N. & Mucci A. (1992). The phosphorus cycle in coastal marine sediments. *Limnology
677 and Oceanography*, 37, 1129-1145.
- 678 Sundby, B., Lecroart, P., Anschutz, P., Katsev, S., & Mucci, A. (2015). When deep diagenesis in Arctic Ocean sediments
679 compromises manganese-based geochronology. *Marine Geology*, 366, 62-68.
- 680 Tyrrell, T. (1999). The relative influences of nitrogen and phosphorus on oceanic primary production. *Nature*,
681 400(6744), 525-531.
- 682 Wallmann, K. (2010). Phosphorus imbalance in the global ocean? *Global Biogeochemical Cycles*, 24(4), GB4030.
683 doi:10.1029/2009GB003643.
- 684 Wallmann, K., Schneider, B. & Sarnthein, M. (2016). Effects of eustatic sea level change, ocean dynamics, and nutrient
685 utilization on atmospheric pCO₂ and seawater composition over the last 130 000 years: a model study. *Climate of the
686 Past*, 12(2), 339-375.

687 Yao, W. & Millero, F.J. (1996). Adsorption of phosphate on manganese dioxide in seawater. Environmental Science &
688 Technology, 30(2), 536-541.

689

690 **Figure captions**

691

692 Figure 1. A simple two-reservoir representation of the oceanic phosphorus cycle.

693

694 Figure 2. Porewater profiles for relevant species ($\text{CH}_4/\text{SO}_4/\text{Fe(II)}/\text{H}_2\text{S}$). Note that the SMT
695 migrates vertically when forced by variable CH_4 fluxes.

696

697

698

699 **Table captions**

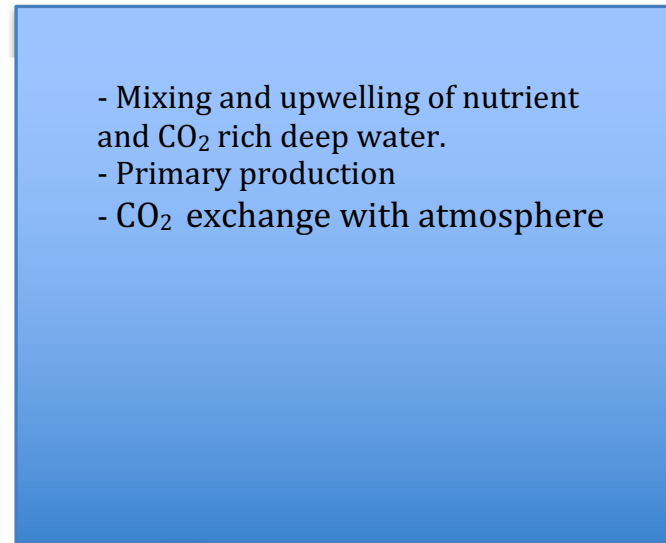
700

701 Table 1. The glacial-interglacial phosphorus cycle: Events and consequences.

702

Figure 1.

Oceanic Reservoir

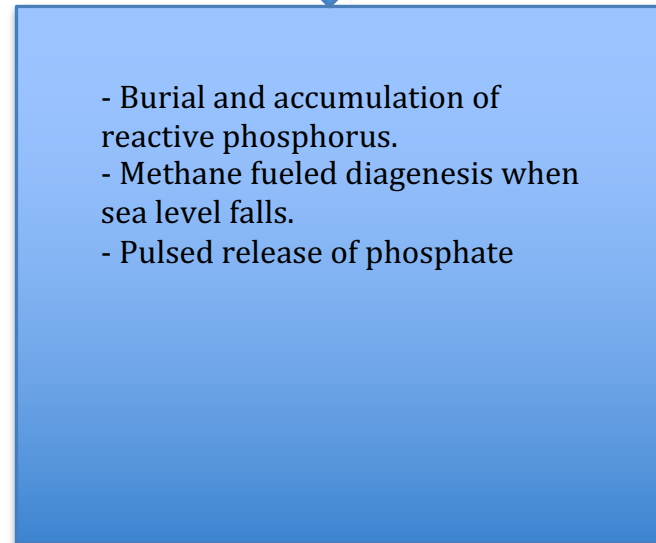


Permanent loss of phosphorus to pelagic sediments

Continental Margin Reservoir



Continental influx of phosphorus

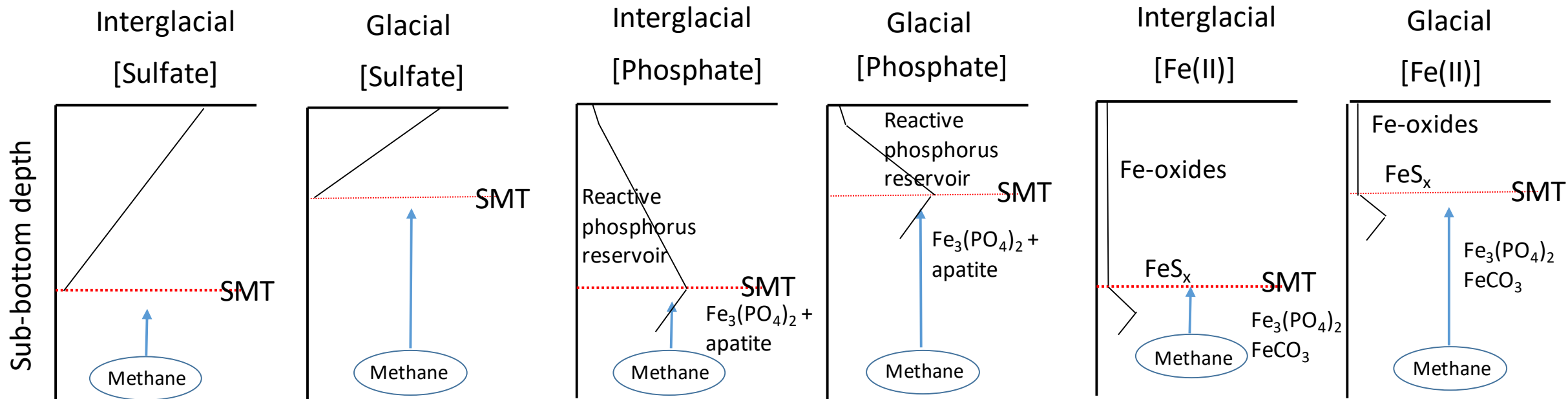


Sedimentation of reactive phosphorus on margins



PO₄ input to the ocean

Figure 2.



EVENTS	IMPACTS	NOTES
1. A glacial cycle begins	Temperature decreases globally, ice builds up on the continents, sea level begins to fall	
2. The pressure on the sea floor decreases	The upper and lower boundaries of the methane hydrate stability field in the sediment column shift upward	
3. Methane hydrate located below the lower stability boundary becomes unstable and decomposes	Methane is released to the pore water, the methane concentration gradient steepens, and the upward methane flux increases	<i>Had the sea level remained stable, methane fuelled diagenesis would nevertheless have taken place and a flux of phosphate—which we call a 'background' flux—would have been delivered to the ocean. This is because the slow upward displacement of the methane hydrate stability field caused by accumulation and burial of sediment would support an upward directed methane flux. The result of sea level fall is therefore to increase the phosphate flux above and beyond the background.</i>
4. Upward diffusing methane encounters downward diffusing sulfate, which increases the rate of anaerobic methane oxidation (AMO) in the sulfate-methane transition zone (SMT)	The SMT moves upward in the direction of the sediment water interface	<i>Methane can also be oxidized using other electron acceptors such as manganese oxides, which would also release adsorbed phosphate to the pore water.</i>
5. Pore-water hydrogen sulfide accumulates at the displaced SMT	Hydrogen sulfide reduces Fe (III) to Fe (II), thereby releasing phosphate associated with Fe oxides into the pore water. A phosphate maximum appears within the SMT, which supports upward and downward fluxes of phosphate. Ferrous sulfide precipitates.	<i>The upper part of the sediment column, located above the methane oxidation zone, contains reactive phosphorus that was delivered and buried during the previous glacial cycle. This accumulated mass of phosphorus is available for conversion to phosphate and may be thought of as a limiting factor controlling the expansion of the oceanic phosphorus inventory during a glaciation cycle.</i>
6. The zone in the sediment column within which phosphate associated with iron oxides can be released expands in the direction of the sea floor	The phosphate concentration gradient steepens and the phosphate flux towards the sediment-water interface and into the ocean increases	<i>The kinetics of iron oxide reduction by H₂S depends on the reactivity of the oxides, which depends on the mineralogy, time since deposition, etc. Sequential analysis of sediments suggests that the most reactive forms of iron oxide occur in the upper part of the sediment column. With time these oxides become exhausted or converted to less reactive forms with depth (time) in the sediment.</i>
7. Nutrients are assimilated by primary producers and incorporated in biomass.	Irrespective of which nutrient is limiting, primary production incorporates nutrient elements in organic matter, which settles to the seafloor and is progressively buried	<i>The part of the export production that reaches the seafloor in the deep abyssal ocean is oxidized aerobically, and the phosphorus it contains is converted to stable poorly soluble minerals such as fluorapatite and is removed from the oceanic phosphorus cycle. Reactive phosphorus in the material that settles on the continental</i>

		<i>margin is available for diagenesis and may be remobilized and returned to the ocean.</i>
8. Phosphate is released into the oceanic surface layer, temporarily decoupling the oceanic P and C cycles	Reduction of Fe oxides in continental margin sediments delivers phosphate to the upper water column. Oxidation of organic matter settling through the abyssal water column enriches deep water in CO ₂ . Oxidation in the underlying sediment converts phosphorus to stable phosphorous minerals	This is supported by observations: global rate of organic matter burial is maximal during the glaciation (Cartapanis et al. 2016); Boyle (1986); Wallmann, (2010)
9. Stratification of the water column breaks down during the termination of the deglaciation, destabilizes the water column, and facilitates vertical mixing. CO ₂ rich bottom water is transported to the surface ocean. Degassing releases CO ₂ to the atmosphere.	CO ₂ rich, nutrient poor water is brought to the surface. This weakens of the biological pump, which would otherwise draw down CO ₂ from the atmosphere. The partial pressure difference would be controlled by the supply of CO ₂ from the deep ocean. The CO ₂ flux would be directed from the ocean to the atmosphere and create a peak in atmospheric CO ₂ .	
10. Upon termination of the glaciation the sea level rises and lowers the pressure on the sea floor.	The fluxes of methane and diagenetically released phosphate become weaker and return to pre-glaciation background levels	